Sub-100-nm Pattern Formation through Selective Chemical Transformation of Self-Assembled Monolayers by Soft X-ray Irradiation

ARTICLE *in* LANGMUIR · APRIL 2003

Impact Factor: 4.46 · DOI: 10.1021/la026815y

8 AUTHORS, INCLUDING:

Young-Hye La
IBM
42 PUBLICATIONS **1,119** CITATIONS
SEE PROFILE

Kyuwook Ihm
Pohang Accelerator Laboratory
42 PUBLICATIONS **454** CITATIONS
SEE PROFILE

Bongsoo Kim
Pohang University of Science and Technology
295 PUBLICATIONS **2,755** CITATIONS
SEE PROFILE

Joon Won Park
Pohang University of Science and Technology
96 PUBLICATIONS **2,154** CITATIONS
SEE PROFILE

Sub-100-nm Pattern Formation through Selective Chemical Transformation of Self-Assembled Monolayers by Soft X-ray Irradiation

Young-Hye La,† Yu Jin Jung,† Hyun Ju Kim,† Tai-Hee Kang,‡ Kyuwook Ihm,‡ Ki-Jung Kim,‡ Bongsoo Kim,‡ and Joon Won Park*,†

Center for Integrated Molecular Systems, Department of Chemistry, Division of Molecular and Life Sciences, Pohang University of Science and Technology, San 31 Hyoja-dong, Pohang, 790-784, Korea, and Pohang Accelerator Laboratory, San 31 Hyoja-dong, Pohang, 790-784, Korea

Received November 7, 2002. In Final Form: February 13, 2003

A new nanopatterning system based on a soft X-ray induced chemical transformation of a nitro-substituted aromatic imine monolayer has been developed. The molecular layer was exposed to soft X-rays, and the involved chemical transformation on the molecular layer was analyzed by using Fourier transform infrared reflection−absorption spectroscopy. As a result, we could confirm that the nitro group on the imine monolayer was cleaved upon the soft X-ray irradiation, leaving the hydrophobic phenyl unit intact on the monolayer surface, while the imine functionality was transformed into a new nonhydrolyzable one. However, the source of the hydrogen atom for the reduction and the final functionality at the para position of the aromatic group are unknown yet. Whereas, we could restore the hydrophilic amine functionality from the unexposed imine monolayer through hydrolysis. These phenomena were applied to the patterning of self-assembled monolayers featuring alternating height, chemical reactivity, and wettability. Alternating surface wettability is evident when water is sprayed on a macroscopically patterned substrate and the plate is tilted to drip the water. Also, atomic force microscope images revealed patterns as small as ≤100 nm with regular height and phase variations. The patterned monolayer was further modified with a linker and Cy3-tagged oligonucleotide, sequentially. Fluorescence images showed that the above molecules were selectively immobilized onto the amine-terminated region of the patterned surface.

I. Introduction

Micro- or nanofabrication, that is, the generation of micro- or nanoscaled structures, has attracted immense interest as the semiconductor industry has developed.[1] It has been a key technology for producing powerful microprocessors and miniaturized high-density memory chips in microelectronics;[2] moreover, it has been also applied to other areas, for example, microelectromechanical systems (MEMS),[3] biotechnology,[4] microanalysis,[5] sensors,[6] and so forth. The patterning required in microfabrication is usually carried out with the photolithographic method employing deep UV radiation and polymer photoresists.[7] However, conventional photolithography is now facing a resolution limitation due to the wavelength of the light source and the line-edge roughness of polymer films.[7a] Therefore, irradiation with shorter wavelengths, such as by extreme UV (EUV),[8] X-ray,[9] electron beam,[10] and ion beam,[11] has been progressively introduced to generate structures with smaller feature sizes below 100 nm.[12] In particular, *extreme UV lithography*, *a projection lithography carried out with radiation from 40 to 1 nm wavelength* (*extreme UV, soft X-ray radiation*), has recently

* To whom correspondence should be addressed. E-mail: jwpark@postech.ac.kr.

† Pohang University of Science and Technology.

‡ Pohang Accelerator Laboratory.

(1) General reviews on nanoscience and nanotechnology: (a) *Science* **1991**, *254*, 1300−1342. (b) Ozin, G. A. *Adv. Mater.* **1991**, *4*, 612−649. (c) Eckardt, L. H.; Naumann, K.; Pankau, W. M.; Rein, M.; Schweitzer, M.; Windhab, N.; von Kiedrowski, G. *Nature* **2002**, *420*, 286. (d) Patzke, G. R.; Krumeich, F.; Nesper, R. *Angew. Chem., Int. Ed.* **2002**, *41* (14), 2446.

(2) (a) Keyes, R. W. *Phys. Today* **1992**, *45* (8), 42. (b) Hide, F.; Díaz-García, M. A.; Schwartz, B. J.; Andersson, M. R.; Pei, Q.; Heeger, A. J. *Science* **1996**, *273*, 1833. (c) Sein, H.; Ahmed, W.; Hassan, I. U.; Ali, N.; Gracio, J. J.; Jackson, M. *J. Mater. Sci.* **2002**, *37* (23), 5057. (d) Keren, K.; Krueger, M.; Gilad, R.; Ben-Yoseph, G.; Sivan, U.; Braun, E. *Science* **2002**, *297*, 72.

(3) (a) Wise, K. D.; Najafi, K. *Science* **1991**, *254*, 1335. (b) Bryzek, J.; Peterson, K.; McCulley, W. *IEEE Spectrum* **1994**, *31* (5), 20. (c) MacDonald, N. C. *Microelectron. Eng.* **1996**, *32*, 49. (d) Kovacs, G. T. A.; Peterson, K.; Albin, M. *Anal. Chem.* **1996**, *68*, 407A. (e) Shipway A. N.; Willner, I. *Acc. Chem. Res.* **2001**, *34* (6), 421.

(4) Recent reviews on combinatorial synthesis: (a) *Chem. Rev.* **1997**, *97* (2), 347−510. (b) Murphy, W. L.; Mooney, D. J. *Nat. Biotechnol.* **2002**, *20* (1), 30.

(5) (a) Service, R. E. *Science* **1995**, *268*, 26. (b) Goffeau, A. *Nature* **1997**, *385*, 202. (c) Burns, M. A. *Science* **2002**, *296*, 1818.

(6) (a) Galla, H.-J. *Angew. Chem., Int. Ed. Engl.* **1992**, *31*, 45. (b) Kleinschmidt, P.; Hanrieder, W. *Sens. Actuators, A* **1992**, *33*, 5. (c) Vellekoop, M. J.; Lubking, G. W.; Sarro, P. M.; Venema, A *Sens. Actuators, A* **1994**, *44*, 249. (d) Bryzek, J. *Sensors* **1996**, *7*, 4. (e) Sun, Y.; Buck, H.; Mallouk, T. E. *Anal. Chem.* **2001**, *73*, 1599.

(7) (a) Okazaki, S. *J. Vac. Sci. Technol., B* **1991**, *9*, 2829. (b) Jeong, H. J.; Markle, D. A.; Owen, G.; Pease, F.; Grenville, A.; von Bünau, R. *Solid State Technol.* **1994**, *37*, 39. (c) Levenson, M. D. *Solid State Technol.* **1995**, *38*, 57. (d) Geppert, L. *IEEE Spectrum* **1996**, *33* (4), 33. (e) Moreau, W. M. In *Semiconductor Lithography*: *Principles and Materials*; Plenum: New York, 1998.

(8) (a) Wood, O. R.; White, D. L.; Bjorkholm, J. E.; Fetter, L. E.; Tennant, D. M.; MacDowell, A. A.; LaFontaine, B.; Kubiak, G. D. *J. Vac. Sci. Technol., B* **1997**, *15* (6), 2448. (b) Bjorkholm, J. E. *Intel Technol. J.* **1998**, *Q3*, 1. (c) Krisch, I.; Choi, P.; Larour, J.; Favre, M.; Rous, J.; Leblanc, C. *Contrib. Plasma Phys.* **2000**, *40* (1−2), 135. (d) Chapman, H. N.; Ray-Chaudhuri, A. K.; Ticher, D. A.; Replogle, W. C.; Stulen, R. H.; Kubiak, G. D.; Rockett, P. D.; Klebanoff, L. E.; O'Connell, D.; Leung, A. H.; Jefferson, K. L.; Wronosky, J. B.; Tayer, J. S.; Hale, L. C.; Blaedel, K.; Spiller, E. A.; Sommargren, G. E.; Folta, J. A.; Sweeney, D. W.; Gullikson, E. M.; Naulleau, P.; Goldberg, K. A.; Boker, J.; Attwood, D. T.; Mickan, U.; Hanzen, R.; Panning, E.; Yan, P.-Y.; Gwyn, C. W.; Lee, S. H. *J. Vac. Sci. Technol., B* **2001**, *19* (6), 2389. (e) Shroff, Y.; Chen, Y.; Oldham, W. *J. Vac. Sci. Technol., B* **2001**, *19* (6), 2412. (f) Hector, S.; Mangat, S. *J. Vac. Sci. Technol., B* **2001**, *19* (6), 2612. (g) Wasson, J. R.; Lu, B.; Mangat, P. J. S.; Nordquist, K.; Resnick, D. J. *J. Vac. Sci. Technol., B* **2001**, *19* (6), 2635.

(9) (a) Moel, A.; Schattenburg, M. L.; Carter, J. M.; Smith, H. I. *J. Vac. Sci. Technol., B* **1990**, *8* (6), 1648. (b) Cerrina, F. *Proc. IEEE* **1997**, *84* (4), 644.

10.1021/la026815y CCC: $25.00
Published on Web 04/05/2003

been promoted as the next generation tool for nanofabrication because this technique is a parallel process in contrast to the serial e-beam writing method.[8b] It has potential for patterning the surface on the scale of several tens of nanometers over a large area. Moreover, in the case of the EUV lithographic system, the size and placement accuracy of the features on the mask are achieved relatively easily because 4:1 reduction is used in the imaging, another advantage distinguishing it from X-ray lithography of 1:1 near-contact printing technology. While the wavelength of the light source is decreased in such a lithographic system, the depth of focus of the light is also reduced. Therefore, the development of a stable, defect-free, ultrathin photoresist is required.[13] In this respect, the utilization of a self-assembled monolayer (SAM) as an imaging layer for EUV lithography has excellent prospects.

SAMs are closely packed molecular assemblies that are chemically bound to metal or metal oxide surfaces.[14] Monolayers of this type are employed not only to control surface properties,[15] such as wettability, adhesion, and lubrication, but also to fabricate new functional materials[16] including catalysts and supports for biomolecules. Above all, SAMs have been considered as ultrathin resists for patterning surfaces with lateral dimensions of several nanometers, because the SAMs have low defect density and their terminal functionality can be controlled on the molecular level.[17]

Therefore, chemical transformation of SAMs by irradiation of X-rays, soft X-rays, EUV, or electron beams is a subject of interest. Recently, Dressick et al. have reported that the *p*,*m*-chloromethylphenyltrichlorosilane (CMPTS) monolayer is attractive for e-beam lithography since it contains an electron-sensitive chloromethyl group. They generated 40-nm-scale patterns on the surface characterized by the displacement of noncovalently bound amine ligands from a CMPTS host film and selective metallization of unirradiated amine-terminated regions.[18] Meanwhile, there are a few reports regarding the bond cleavage or damage of SAMs induced by X-ray or soft X-ray irradiation while taking X-ray photoelectron spectra.[19−21] Whitesides et al. investigated damage to CF_3CO_2- and CF_3CONH-terminated monolayers and demonstrated that photoelectrons ejected from the surfaces, rather than incident X-ray photons, were largely responsible for the damage.[20] Sagiv et al. applied Fourier transform infrared (FT-IR) spectroscopy to obtain a sensitive assessment of damage to hydrocarbon monolayers.[21]

Monolayer damage caused by X-ray irradiation is likely to be selective for a particular functional group. In that case, X-ray irradiation damage would be associated with specific chemical reactions that transform functional groups into new ones. Such transformations can be also used to tailor surface properties with spatial resolution.[22] Nealey et al. pioneered the generation of nanoscale patterns on surfaces using these phenomena. Recently, they found that hydroxy and aldehyde groups were incorporated onto the surface of the methyl-, vinyl-, and trifluoroacetoxy-terminated SAMs when the monolayers were exposed to soft X-rays in the presence of oxygen. They applied these chemical transformations to patterning SAMs with sub-100-nm lateral dimensions.[23]

Previously, we also observed that the carbon−nitrogen bond in nitro-substituted aromatic imine monolayers was cleaved selectively upon soft X-ray irradiation and that the cleavage was efficient with a low dosage.[24] The cleavage accompanies secondary reactions that transform the imine functionality into a nonhydrolyzable one.[24d] However, the chemical properties of the nitro-cleaved imine layers and the photoinduced reaction mechanism for the layers still remain unclear. In this study, we unambiguously characterize the structural change of a nitro-substituted imine monolayer induced by soft X-ray irradiation using Fourier transform infrared reflection−absorption spectroscopy (FT-IRRAS) analysis and report a method of developing sub-100-nm patterns showing alternating height, chemical reactivity, and wettability through the soft X-ray induced chemical transformation of the layers.

(10) (a) Lercel, M. J.; Tiberio, R. C.; Chapman, P. F.; Craighead, H. G.; Sheen, C. W.; Parikh, A. N.; Allara, D. L. *J. Vac. Sci. Technol., B* **1993**, *11* (6), 2823. (b) Lercel, M. J.; Redinbo, G. F.; Pardo, F. D.; Rooks, M.; Tiberio, R. C.; Simpson, P.; Craighead, H. G.; Sheen, C. W.; Parikh, A. N.; Allara, D. L. *J. Vac. Sci. Technol., B* **1994**, *12* (6), 3663. (c) Lercel, M. J.; Rooks, M.; Tiberio, R. C.; Craighead, H. G.; Sheen, C. W.; Parikh, A. N.; Allara, D. L. *J. Vac. Sci. Technol., B* **1995**, *13* (3), 1139. (d) Carr, D. W.; Lercel, M. J.; Whelan, C. S.; Craighead, H. G.; Seshadri, K.; Allara, D. L. *J. Vac. Sci. Technol., A* **1997**, *15* (3), 1446. (e) Hatzor, A.; Weiss, P. S. *Science* **2001**, *291*, 1019. (f) Werts, M. H. V.; Lambert, M.; Bourgoin, J.-P.; Brust, M. *Nano Lett.* **2002**, *2* (1), 43. (g) Geyer, W.; Stadler, V.; Eck, W.; Gölzhäuser, A.; Grunze, M.; Sauer, M.; Weimann, T.; Hinze, P. *J. Vac. Sci. Technol., B* **2001**, *19* (6), 2732.

(11) (a) Chappert, C.; Bernas, H.; Ferré, J.; Kottler, V.; Jamet, J.-P.; Chen, Y.; Cambril, E.; Devolder, T.; Rousseaux, F.; Mathet, V.; Launois, H. *Science* **1998**, *280*, 1919. (b) Facsko, S.; Dekorsy, T.; Koerdt, C.; Trappe, C.; Kurz, H.; Vogt, A.; Hartnagel, H. L. *Science* **1999**, *285*, 1551. (c) Satriano, C.; Conte, E.; Marletta, G. *Langmuir* **2001**, *17*, 2243.

(12) (a) Bruning, J. H. *Solid State Technol.* **1998**, *41*, 59. (b) Burggraaf, P. *Solid State Technol.* **2000**, *43*, 31.

(13) Dressick, W. J.; Calvert, J. M. *Jpn. J. Appl. Phys.* **1993**, *32*, 5829.

(14) (a) Ulman A. *An Introduction to Ultrathin Organic Films from Langmuir−Blodgett to Self-Assembly*; Academic: New York, 1991. (b) Ulman A. *Chem. Rev.* **1996**, *96*, 1533−1554.

(15) (a) Plueddemann, E. P. *Silane Coupling Agents*; Plenum: New York, 1991. (b) Freeman, R. G.; Grabar, K. C.; Allison, K. J.; Bright, R. M.; Davis, J. A.; Guthrie, A. P.; Hommer, M. B.; Jackson, M. A.; Smith, P. C.; Walter, D. G.; Natan, M. J. *Science* **1995**, *267*, 1629. (c) Bhushan, B.; Israelachvili, J. N.; Landman, U. *Nature* **1995**, 374, 607. (d) Eckhardt, C. J.; Peachey, N. M.; Swanson, D. R.; Takacs, J. M.; Khan, M. A.; Gong, X.; Kim, J.-H.; Wang, J.; Uphaus, R. A. *Nature* **1993**, *362*, 614. (e) Sagiv, J. *J. Am. Chem. Soc.* **1980**, *102* (1), 92.

(16) (a) Lee, K. B.; Park, S.-J.; Mirkin, C. A.; Smith, J. C.; Mrksich, M. *Science* **2002**, *295*, 1702. (b) Müller, W. T.; Klein, D. L.; Lee, T.; Clarke, J.; McEuen, P. L.; Schultz, P. *Science* **1995**, *268*, 272. (c) Bhatia, S. K.; Hickman, J. J.; Liger, F. S. *J. Am. Chem. Soc.* **1992**, *114*, 4432. (d) Yang, Z.; Galloway, J. A.; Yu, H. *Langmuir* **1999**, *15*, 8405.

(17) (a) Xia, Y.; Whitesides, G. M. *Angew. Chem., Int. Ed.* **1998**, *37*, 551. (b) Yitzchaik, S.; Marks, T. J. *Acc. Chem. Res.* **1996**, *29*, 197. (c) Gorman, C. B.; Carroll, R. L.; He, Y.; Tian, F.; Fuierer, R. *Langmuir* **2000**, *16*, 6312. (d) Dulcey, C. S.; Georger, J. H., Jr.; Krauthamer, V.; Stenger, D. A.; Fare, T. L.; Calvert, J. M. *Science* **1991**, *26*, 551.

(18) Dressick, W. J.; Chen, M.-S.; Brandow, S. L.; Rhee, K. W.; Shirey, L. M.; Perkins, F. K. *Appl. Phys. Lett.* **2001**, *78* (5), 676.

(19) (a) Rieke, P. C.; Baer, D. R.; Fryxell, G. E.; Engelhard, M. H.; Porter, M. S. *J. Vac. Sci. Technol., A* **1993**, *11*, 2292. (b) Heister, K.; Zharnikov, M.; Grunze, M.; Johansson, L. S. O.; Ulman, A. *Langmuir* **2001**, *17*, 8.

(20) (a) Graham, R. L.; Bain, C. D.; Biebuyck, H. A.; Laibinis, P. E.; Whitesides, G. M. *J. Phys. Chem.* **1993**, *97*, 9456. (b) Laibinis, P. E.; Graham, R. L.; Biebuyck, H. A.; Whitesides, G. M. *Science* **1991**, 254, 981.

(21) Frydman, E.; Cohen, H.; Maoz, R.; Sagiv, J. *Langmuir* **1997**, *13*, 5089.

(22) (a) Suh, D.; Simons, J. K.; Taylor, J. W.; Koloski, T. S.; Calvert, J. M. *J. Vac. Sci. Technol., B* **1993**, *11* (6), 2850. (b) Dressick, W. J.; Dulcey, C. S.; Brandow, S. L.; Witschi, H.; Nealey, P. F. *J. Vac. Sci. Technol., B* **1999**, *17* (4), 1432. (c) Yang, X. M.; Peters, R. D.; Kim, T. K.; Nealey, P. F. *J. Vac. Sci. Technol., B* **1999**, *17* (6), 3203.

(23) (a) Kim, T. K.; Yang, X. M.; Peters, R. D.; Shon, B. H.; Nealey, P. F. *J. Phys. Chem. B* **2000**, *104*, 7403. (b) Yang, X. M.; Peters, R. D.; Kim, T. K.; Nealey, P. F.; Brandow, S. L.; Chen, M.-S.; Shirey, L. M.; Dressick, W. J. *Langmuir* **2001**, *17*, 228.

(24) (a) La, Y.-H.; Kim, H. J.; Maeng, I. S.; Jung, Y. J.; Kang, T.-H.; Kim, K.-J.; Kim, B.; Park, J. W. *Langmuir* **2002**, *18*, 2430. (b) La, Y.-H.; Kim, H. J.; Maeng, I. S.; Jung, Y. J.; Kang, T.-H.; Kim, K.-J.; Ihm, K.; Kim, B.; Park, J. W. *Langmuir* **2002**, *18*, 301. (c) Moon, J. H.; La, Y.-H.; Shim, J. Y.; Hong, B. J.; Kim, K.-J.; Kang, T.-H.; Kim, B.; Kang, H.; Park, J. W. *Langmuir* **2000**, *16*, 2981. (d) Moon, J. H.; Kim, K.-J.; Kang, T.-H.; Kim, B.; Kang, H.; Park, J. W. *Langmuir* **1998**, *14*, 5673.

II. Experimental Section

Materials. The silane coupling agent, (3-aminopropyl)diethoxymethylsilane (APDES), was purchased from Gelest, Inc., and 11-amino-1-undecanethiol·hydrochloride was purchased from Dojindo Laboratories. 4-Nitrobenzaldehyde and 4-nitrocinnamaldehyde were purchased from Aldrich Chemical Co. and used as received. The polished prime Si(100) wafers (dopant, phosphorus; resistivity, 1.5−2.1 Ω·cm) were purchased from MEMC Electronic Materials, Inc. Gold-coated substrates prepared by electron-beam deposition of 10 nm of Ti followed by 200 nm of Au onto Si(100) wafers were purchased from Lance Goddard Associates (Foster City, CA). A heterobifunctional linker, succinimidyl 4-maleimido butyrate (SMB), was synthesized as described in the literature.[25] Thiol-tethered oligonucleotide having a Cy3 fluorescence tag (3′-SH-spacer-ACCTG-Cy3-5′) was purchased from Cruachem, Ltd. The zone plate (diameter, 120 μm; line width of outer zones, 80 nm) and copper TEM grid (type: G2150C, 150 mesh) were purchased from Gate Micro Technology (Italy) and Agar Scientific (U.K.), respectively.

Preparation of Nitro-Substituted Aromatic Imine Monolayers. For the preparation of 4-nitrobenzaldimine and 4-nitrocinnamaldimine monolayers, the amine-terminated substrates (aminosilyated silicon wafer[26] or aminothiolated gold[27]) were immersed into anhydrous ethanol solution (20 mL) containing 4-nitrobenzaldehyde (ca. 10 mg) and 4-nitrocinnamaldehyde (ca. 10 mg) under a nitrogen atmosphere, respectively. The aldehyde derivatives were condensed with amines of the APDES monolayer at 50 °C for 6 h. After the condensation, the substrates were sonicated in ethanol, acetone, and dichloromethane, sequentially. For each sonication step, 2 min was allowed (for gold substrate, 30 s was allowed). Finally, the substrates were dried under vacuum. Thus formed aromatic imine substrates were stored in a vial under vacuum, and the substrates were transferred into an ultrahigh vacuum (UHV) chamber of the synchrotron beam line for soft X-ray exposure.

Patterning of Nitro-Substituted Aromatic Imine Monolayers by Soft X-rays. The patterning experiment was carried out at the 4B1 PEEM (photoemission electron microscopy) beamline of Pohang Accelerator Laboratory (Korea). The photon flux measured at the energy of 550 eV was 6.6×10^{11} photons/cm^2·s. The nitro-aromatic monolayers were irradiated through a photomask in close proximity to the surface (gap, below 5 μm) with a dosage from 50 to 139 mJ/cm^2 (the energy of 550 eV, the total dosage used in the patterning was selected individually for the best contrast.[24a]). After irradiation, samples were hydrolyzed in 0.2% aqueous acetic acid solution for 5 min and sonicated for 1 min in water and methanol, sequentially. Finally, the samples were dried under vacuum.

Immobilization of Cy3-Tagged Oligonucleotide on the Patterned Surfaces. The patterned molecular layers were treated for 3 h with a solution of succinimidyl 4-maleimido butyrate (c = 20 mM) dissolved in sodium bicarbonate buffer (50 mM, pH 8.5). (The solution was prepared by dissolving 56 mg of succinimidyl 4-maleimido butyrate in DMF (1.0 mL) and then diluting 10-fold with the buffer.) After incubation, the substrate was washed several times with deionized water and dried under vacuum. Subsequently, linker-modified substrates were dipped into stock solutions (c = 200 μM) of the thiol-tethered oligodeoxynucleotide (3′-SH-spacer-ACCTG-Cy3-5′) in HEPES buffer (10 mM, pH 6.6, 5.0 mM EDTA). (Right before the reaction, the stock solutions were pretreated with DTT (dithiothreitol) to cleave the disulfide linkage and prohibit the further formation of the disulfide. Subsequently, repeated extraction with ethyl acetate was performed in order to remove excess DTT.) After the reaction, the substrates were washed with the hybridization buffer (hybridization buffer: sodium dodecyl sulfate buffer solution (c = 7.0 mM, pH 7.4) dissolving NaCl (300 mM), sodium phosphate (20 mM), and EDTA (2 mM)) and dried under vacuum.

(25) (a) Partis, M. D.; Griffiths, D. G.; Roberts, G. C.; Beechey, R. B. *J. Protein Chem.* **1983**, *2*, 263. (b) Reddy, P. Y.; Kondo, S.; Fujita, S.; Toru, T. *Synthesis* **1998**, *7*, 999.

(26) (a) Moon, J. H.; Kim, J. H.; Kim, K.-J.; Kang, T.-H.; Kim, B.; Kim, C.-H.; Hahn, J. H.; Park, J. W. *Langmuir* **1997**, *13*, 4305. (b) Moon, J. H.; Shin, J. W.; Kim, S. Y.; Park, J. W. *Langmuir* **1996**, *12*, 4621.

(27) Tien, J.; Terfort, A.; Whitesides, G. M. *Langmuir* **1997**, *13*, 5349.

Scheme 1. Formation of Nitro-Aromatic Imine Monolayers

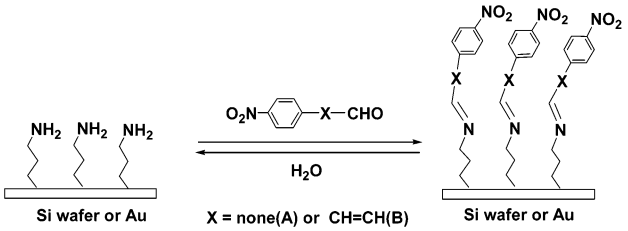

FT-IRRAS Analysis. Surface FT-IR spectra were recorded using a Bruker IFS 66v FT-IR spectrometer equipped with an MCT detector and an A513 variable angle reflection accessory. p-Polarized light at an incidence angle of 80° was used, and the spectra were collected from 1024 scans at 4 cm^{-1} resolution.

Atomic Force Microscopy (AFM) Analysis. AFM images were obtained using a AutoProbe CP Research atomic force microscope (Park Scientific Instruments). Data were acquired in the contact mode and analyzed using ProScan software.

Fluorescence Scanning. A commercial confocal laser scanner, ScanArray Lite (GSI Lumonics), and quantitative microarray analysis software, QuantArray (GSI Lumonics), were used for image acquisition and display.

Pictures of Water Wetting. Photographs of water wetting were obtained using a high-performance digital camera (model, HAMAMATSU C4742; resolution, 1024 × 1024).

III. Results and Discussion

Nitro-substituted aromatic imine monolayers used in this study were prepared by treating aminosilanized silicon wafers and aminothiolated gold substrates with relevant aromatic aldehydes (4-nitrobenzaldehyde, **A**, and 4-nitrocinnamaldehyde, **B**) (Scheme 1).

The aminosilanized and aminothiolated layers were obtained by allowing silicon wafers and gold substrates to react with APDES[26] and 11-amino-1-undecanethiol·hydrochloride,[27] respectively. The imine formation is complete in 3 h in the presence of a large excess of the nitro-aromatic aldehyde, and the hydrolysis of the thus formed imine monolayer restores the surfaces to hydrophilic amine functionality,[26] which is one of the important chemical properties that generates a reactive nanopattern on our monolayer surface. The thickness of the imine monolayers on silicon wafers was typically 12 and 14 Å for 4-nitrobenzaldimine (from **A**) and 4-nitrocinnamaldimine (from **B**) monolayers, respectively. The absolute density of the imines on the silicon surface was determined to be ca. 4 imines/nm^2 for each monolayer.[26a] Gold substrates were used for the external reflection FT-IR analysis because they have higher reflectivity than silicon wafers for IR spectral sensitivity.

Selective Chemical Transformation of the Monolayers by Soft X-ray Irradiation. To scrutinize the chemical transformations of the 4-nitrobenzaldimine monolayer caused by soft X-ray irradiation, the whole area (1 × 3 cm) of a monolayer on a gold substrate was irradiated, and the resulting molecular layer was analyzed with FT-IRRAS. To ensure uniform exposure to the soft X-rays over the whole area, the position of the beam (beam size = 0.8 × 8 mm) was shifted 0.8 mm after irradiation to 18 mJ/cm^2 dosage. Parts a and b of Figure 1 show FT-IR spectra of a 4-nitrobenzaldimine monolayer on a gold substrate before and after exposure to the 550 eV (corresponding wavelength, 2.3 nm) soft X-rays, respectively. In Figure 1, only the spectral range of interest is presented. Before irradiation, the spectrum shows absorption bands associated with the nitrobenzaldimine unit, that is, C═N, aromatic C═C, asymmetric, and symmetric NO_2 stretching vibrations located at 1646, 1603, 1524,

Scheme 2. Patterning Procedure of the Imine Monolayers by Soft X-rays[a]

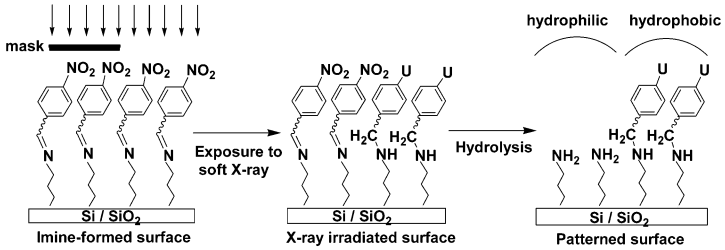

[a] U, functional group(s) from the cleavage.

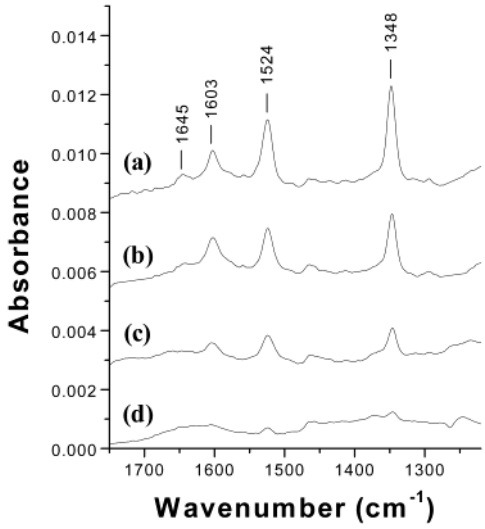

Figure 1. FTIR spectra of a 4-nitrobenzaldimine monolayer on a gold substrate. Each spectrum is obtained (a) before irradiation, (b) after irradiation by soft X-rays (550 eV, 18 mJ/cm^2), (c) after hydrolysis of the irradiated sample, and (d) after hydrolysis of the unexposed sample. Spectra were recorded using p-polarized light at an incidence angle of 80° (scan numbers,1024; resolution, 4 cm^{-1}).

and 1348 cm^{-1}, respectively.[28] After irradiation, the C═N stretching vibration peak of the imine moiety and the NO_2 asymmetric/symmetric stretching vibration peaks were reduced to about 57% and 36% of the original values, respectively, but the aromatic C═C stretching vibration peak was almost invariant.[29] This observation shows that the nitro group on the benzaldimine monolayer is cleaved selectively upon soft X-ray irradiation, leaving the phenyl unit intact on the monolayer surface and transforming the imine functionality into new chemical species. The former selectivity is in harmony with the X-ray photoelectron spectroscopy results reported previously,[24] and the latter chemical transformation was hinted at by the previous wet analysis of the irradiated sample.[24d]

To determine molecular changes involved in the photoreaction, the irradiated sample was dipped into deionized water to hydrolyze the intact imine bond. Figure 1c shows the IR spectrum of the hydrolyzed sample. The remaining C═N absorption peak (about 43% of the original value) disappeared completely after the hydrolysis, while over 40% of the C═C absorption peak of the aromatic unit remained. In addition, more than 30% of asymmetric and symmetric NO_2 absorption peaks still survived the hydrolysis. Therefore, it is clear that the phenyl unit is left on the surface, and a part of the phenyl still retains the nitro group. To find out whether the remaining NO_2 absorption peaks arise from the incomplete hydrolysis of the imine moiety, the reaction time was increased. However, the same spectrum was obtained. As shown in Figure 1d, only trace amounts of aromatic C═C and nitro absorption bands are observed after hydrolysis of the unirradiated 4-nitrobenzaldimine monolayer. Therefore, it is clear that the nitro absorption peaks presented in Figure 1c arise from the nitro-phenyl moiety; the imine bond is transformed into a nonhydrolyzable species. This result implies that cleavage of the nitro group induces the transformation of the imine bond not only of the molecule but also of the vicinity of the particular molecule undergoing the cleavage.

Previously, we have analyzed the molecules remaining on the irradiated surface with gas chromatography−mass spectrometry (GC−MS) coupled with a solid-phase microextraction (SPME) method that was performed after hydrolyzing the imine bond. The analysis suggests that the nitro group cleavage was accompanied by secondary reactions that transformed the imine functionality into a nonhydrolyzable one.[24d] The current FT-IR analysis is totally in harmony with the previous wet analysis. However, the source of the hydrogen atom for the reduction and the final functionality at the para position of the aromatic group are unknown yet.

Nanopattern Formation of the Monolayers by Soft X-rays. Irradiating the nitro-substituted aromatic imine monolayers by soft X-rays successfully provides a pattern featuring alternating height, chemical reactivity, and wettability. The patterning procedure is presented in Scheme 2.

4-Nitrobenzaldimine and 4-nitrocinnamaldimine monolayers on silicon wafers were exposed to synchrotron soft X-rays of 550 eV with dosages of 139 and 98 mJ/cm^2, respectively: the nitro groups in the nitrocinnamaldimine monolayer are more efficiently cleaved than those in the nitrobenzaldimine layer.[24a] The beam was passed through a photomask in close proximity to the surface with an angle of 90° to the substrate. A zone plate, consisting of engraved gold concentric circles with varying line widths from 264 to 80 nm on a silicon nitride membrane, was used as the mask. After irradiation, samples were hydrolyzed in deionized water containing catalytic amounts of acetic acid. As mentioned above, the nitro groups of the exposed regions were cleaved, and the imine functionalities were transformed into hydrophobic, nonhydrolyzable ones. The secondary amines shown in Scheme 2 represent hypothesized functional groups most likely to be formed as a result of imine reduction in this system. However, monolayers unexposed to the soft X-rays were intact, and the hydrolysis restored the surfaces to hydrophilic amine functionality. Hence, a height difference between the exposed and unexposed regions of the molecular layers

(28) Socrates, G. In *Infrared Characteristic Group Frequencies*: *Tables and Charts*, 2nd ed.; John Wiley & Sons Ltd: New York, 1994. In particular, the imine (C═N) absorption peak at 1646 cm^{-1} was confirmed by comparing the 4-nitrobenzamide monolayer in which an amide bond connects the 4-nitrophenyl group to the propylsiloxane surface.

(29) For quantitative analysis of the chemical transformation, the band area was numerically calculated with a linear background subtraction.

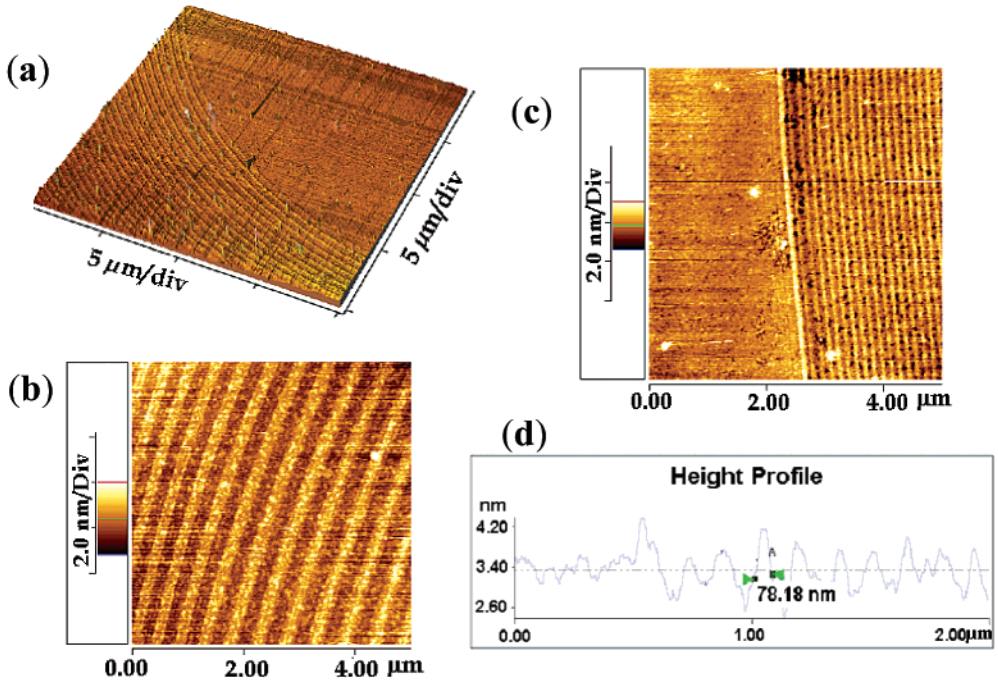

Figure 2. AFM topographic images of the patterned nitro-aromatic imine monolayers on silicon wafers: (a) 4-nitrocinnamaldimine monolayer (scan size: 20 μm × 20 μm, 3-D); (b,c) inner zones and outer zones of the zone plate transferred onto a 4-nitrobenzaldimine monolayer (scan size, 5 μm × 5 μm); (d) the height profile of image c.

was generated. The difference in topography on the patterned surfaces was directly observed by AFM.

A large-scale 3-D image of a patterned nitrocinnamaldimine monolayer is shown in Figure 2a. Also, parts b and c of Figure 2 display the inner and outer zones of the zone plate imaged onto a nitrobenzaldimine monolayer, respectively. As shown in these AFM images, features of the zone plate containing various line widths were successfully transferred onto the imine monolayers (line widths are diminished upon moving to the left side of the images), and the line edges in the patterns appeared clear even for the smallest line of the outer zones. The line width measured by AFM is about 78 nm in the outer zones, which is quite consistent with the reported feature size (80 nm) of the zone plate (Figure 2d). The height differences between the exposed (bright) and the unexposed (dark) regions are 7−8 Å for the nitrocinnamaldimine monolayer and 5−6 Å for the nitrobenzaldimine monolayer. The result well demonstrates that we can control the height difference on a patterned surface by modifying the length of aldehyde molecules used in the imine formation.

To verify the role of the nitro group in the patterning process, an unsubstituted benzaldimine monolayer was also examined in the same condition. The pattern was not observed on it. This control experiment shows that the nitro group plays an important role in the pattern formation. That is, it clearly supports the proposed mechanism that the nitro group cleavage induces (or facilitates) the chemical transformation of the imine bond.

While light of 550 eV was employed for this particular pattern formation, we observed that the nitro group was also cleaved efficiently with a beam of even lower energy (<100 eV; wavelength of 12 nm; EUV region). Therefore, successful patterning of the monolayer using extreme UV (10−14 nm) radiation is also expected.

Selective Immobilization of the Oligonucleotide on the Patterned Surfaces. Amine-functionalized self-assembled monolayers can bind various functional materials, such as enzymes, antibodies, and inorganic

Scheme 3. Immobilization Process of the Linker Molecule (SMB) and a Cy3-Tagged Oligonucleotide on the Patterned Surface

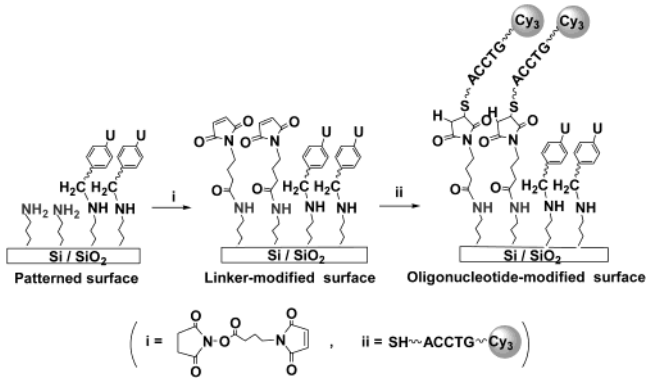

catalysts, through covalent or ionic bond formation.[30] We examined whether our patterned surface is suitable for a template for the selective immobilization of such functional molecules. A 4-nitrocinnamaldimine monolayer on a silicon wafer was irradiated through a 150-mesh TEM grid with a dosage of 98 mJ/cm^2, and the patterned surface was hydrolyzed immediately. The patterned monolayer was treated in a sequential manner with a heterobifunctional linker, SMB, and a thiol-tethered oligonucleotide having a Cy3 fluorescence tag (3′-SH-spacer-ACCTG-Cy3-5′) (Scheme 3).

Figure 3 shows a fluorescence image of the oligonucleotide immobilized on the patterned nitrocinnamaldimine monolayer. For the patterning, the beam (0.8 mm × 5 mm) was focused on the center part of the TEM grid (150 mesh). An optical microscope showed that the line width of the employed grid was 40 μm. The unexposed regions with the restored amine functionality appear bright (green

(30) (a) Wirth, M. J.; Fairbank, R. W. P.; Fatunmbi, H. O. *Science* **1997**, *275*, 44. (b) Bianco, A.; Gasparrini, F.; Maggini, M.; Misiti, D.; Polese, A.; Prato, M.; Scorrano, G.; Toniolo, C.; Villani, C. *J. Am. Chem. Soc.* **1997**, *119*, 7550. (c) Yang, Z.; Yu, H. *Langmuir* **1999**, *15*, 1731.

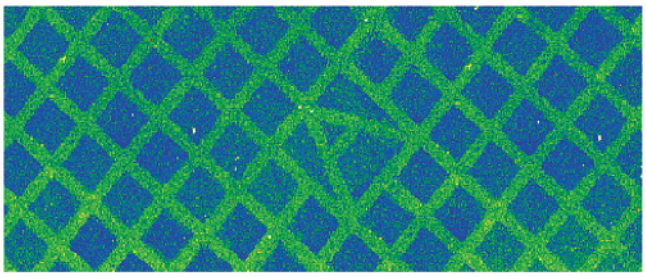

Figure 3. Fluorescence image of the patterned nitrocinnamaldimine monolayer treated with a Cy3-tagged oligonucleotide. The bright regions (green artificial color) of the image are unexposed spots where the oligonucleotide is selectively immobilized. In the center, the character A transferred from the TEM grid is evident.

artificial color), and the contrast between the exposed and the unexposed regions is very clear (the average intensity ratio is 1.8:1.0). This observation clearly confirms the expectation that the amine groups on the patterned surface are still reactive after going through the patterning process. As a result, the Cy3-tagged oligonucleotide is selectively immobilized on the amine-terminated regions. Such a patterning methodology is expected to find many applications in high-density biochips and miniaturized bio- (or chemical) sensors.

Alternating Wettability of Exposed and Unexposed Regions. The wettability test is a convenient way to verify the nature of molecular layers. To identify the difference in wetting behaviors between an exposed 4-nitrobenzaldimine monolayer and a restored monolayer of the amine functionality, the sample on gold was irradiated with a spatial interval of 1.5 mm, and the position of the beam (beam size = 0.8 mm × 8 mm) was shifted after irradiation to 59 mJ/cm^2 dosage to cleave the nitro group extensively.[31] After irradiation and hydrolysis, water was sprayed on the dry surface. Figure 4 shows the wetting behavior and an evident formation of bands. The bright bands are formed because water droplets reflect the light. The dark regions that were exposed to soft X-rays repel water due to their hydrophobicity. This result again supports the conclusion that the irradiated nitrobenzaldimine layers have been changed into nonhydrolyzable and hydrophobic surfaces. This method of controlling the wettability of a monolayer with soft X-rays might find application in the self-assembly of metals or block copolymers essential for nanoresist formation.

IV. Conclusion

We have shown that irradiating the nitro-aromatic imine monolayer by soft X-rays (i.e., EUV) can provide a pattern featuring alternating height, chemical reactivity, and wettability on sub-100-nm dimensions. Since the wavelength of the light source employed in the patterning process is one of the important factors determining the resolution, use of soft X-rays for nanofabrication is a timely choice that overcomes the resolution limit of the conventional deep UV (193 nm) system.

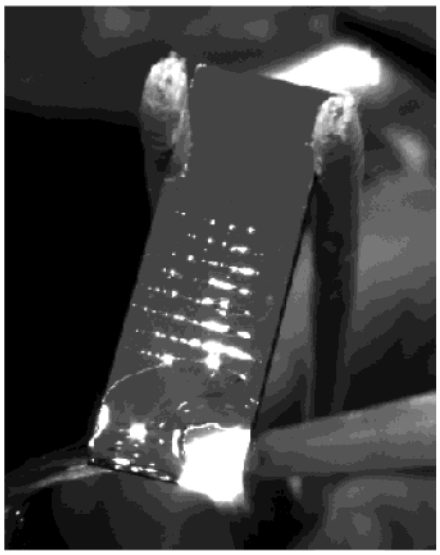

Figure 4. A photograph showing water wetting characteristics of a macroscopically patterned 4-nitrobenzaldimine monolayer. The sample is irradiated at intervals of 1.5 mm; the position of the beam (beam size = 0.8 mm × 8 mm) was shifted after irradiation to 59 mJ/cm^2 dosage. Nine different periodic positions on the sample were irradiated.

The 80-nm resolution demonstrated in this study was governed by the resolution of the mask available for this study. We believe that use of an appropriate mask and related hardware optimization will allow patterning of a sub-50-nm structure with sharp edges. Our patterning system using SAMs as an ultrathin imaging layer that is sensitive to soft X-rays seems to be most suitable for realizing high-resolution patterning for biotechnology applications. In particular, nitro-aromatic SAMs are very sensitive to soft X-ray irradiation, since the dosage required for the pattern fabrication is relatively low (50−140 mJ/cm^2 at 550 eV) compared to that for other monolayer systems such as alkanesilanes (optimum dosage for octadecyltrichlorosilane, 1000 mJ/cm^2 at 1240 eV).[23] Importantly, the reactive amine functionality that can bind the various functional moieties (for example, nanoparticles, metal, biomolecules, etc.) remains on the patterned surfaces.

Acknowledgment. Student fellowships of Brain Korea 21 are greatly acknowledged, and the work is also supported by the Korea Science and Engineering Foundation through the Center for Integrated Molecular Systems and the Korea Research Foundation (KRF-1998-005-E00309). Experiments at the Pohang Light Source (PLS) were supported in part by the Ministry of Science and Technology and POSCO.

LA026815Y

(31) Notes: The nitro groups on a gold substrate are more efficiently cleaved than those on a silicon wafer. This difference of cleavage rate is reminiscent of earlier results reported by Whitesides, whose team studied X-ray-promoted damage of CF_3CO_2-terminated monolayers on various substrates; upon the irradiation, the substrates that ejected electrons less efficiently exhibited a slower loss rate of fluorine from the SAMs. They demonstrated that photoelectrons ejected from the surface are largely responsible for the damage (ref 20b).